J. Fluid Mech. (2006), *vol.* 546, *pp.* 295–311.
doi:10.1017/S0022112005007159 Printed in the United Kingdom

Natural convection in a stably stratified fluid along vertical plates and cylinders with temporally periodic surface temperature variations

By ALAN SHAPIRO AND EVGENI FEDOROVICH

School of Meteorology, University of Oklahoma, Norman, OK 73019, USA

(Received 27 October 2004 and in revised form 27 May 2005)

This paper describes one-dimensional (parallel) laminar natural convection in a viscous stably stratified fluid owing to temporally periodic variations in the surface temperature of infinite vertical plates and circular cylinders. Analytical solutions of the one-dimensional (parallel) Boussinesq equations of motion and thermodynamic energy are obtained for the periodic regime for arbitrary values of ambient stratification, Prandtl number and forcing frequency. The solutions for plates and cylinders are qualitatively similar and show that (i) the flows are composed of two waves that decay exponentially with distance from the surface: a fast long wave and a slow short wave; (ii) for forcing frequencies greater than the natural frequency of the corresponding inviscid system, these two waves propagate away from the surface; and (iii) for forcing frequencies less than this natural frequency, the short wave propagates away from the surface while the long wave propagates toward the surface. This latter case provides an example of a flow for which the conventional radiation condition is not appropriate. The analytical results are complemented, for the plate problem, with three-dimensional numerical simulations of flows that start from rest and are suddenly subjected to a periodic thermal forcing at the plate. The numerical results depict the transient (start-up) stage of the flow and the approach to a periodic regime. These results confirm that the analytical solutions provide the appropriate description of the periodic regime.

1. Introduction

Unsteady natural convection flows abound in nature and technology. Such flows are notoriously difficult to analyse theoretically because of the intrinsic coupling between the temperature and velocity fields. A notable exception is the classical problem of unsteady laminar one-dimensional (parallel) natural convective flows along an infinite vertical plate, a class of flows for which the Boussinesq equations of motion and thermodynamic energy reduce to a set of linear partial differential equations that may be solved analytically in a number of circumstances (Gebhart *et al.* 1988). These solutions can be counted among the few known exact solutions of unsteady natural convection. Such solutions are prized for the insights they provide into flow behaviour and for their use as benchmark solutions for verification of computational fluid dynamics algorithms.

In the 1950s and 1960s, analytical solutions for unsteady one-dimensional natural convection along an infinite vertical plate were obtained for a variety of surface

forcings, for an unstratified fluid (Illingworth 1950; Siegel 1958; Menold & Yang 1962; Schetz & Eichhorn 1962; Goldstein & Briggs 1964). The related problem of unsteady natural convection from an impulsively heated circular cylinder was considered by Goldstein & Briggs (1964). These solutions described resting fluids that were abruptly set into motion through the agency of a surface heat flux or temperature perturbation of prescribed temporal variation. The flows were characterized by a sudden burst of convection along the plate, followed by an inexorable outward growth of the boundary layer. One-dimensional solutions were obtained for natural convection driven by impulsively started temporally periodic surface temperature and surface heat flux variations of vertical plates (Das, Deka & Soundalgekar 1999; Soundalgekar, Deka & Das 2003). The asymptotic solution for convection driven by temporally periodic surface heating (purely periodic regime after transients had damped out) was considered by Schetz & Eichhorn (1962). The corresponding purely periodic regime for convection in circular ducts was considered by Barletta & di Schio (2004).

Laboratory experiments of natural convection of unstratified fluid along vertical plates subject to an impulsive heat flux showed that the one-dimensional solution provided an appropriate description of the transient flow in regions where the disturbance arising from the presence of the leading edge of the plate had not yet propagated (Gebhart *et al.* 1988, and references therein). The one-dimensional framework was also found to apply at the early stages of natural convection in rectangular cavities with heated/cooled sidewalls (Schladow 1990; Armfield & Patterson 1992; Schöpf & Patterson 1995). However, recent studies suggest that before the arrival of this leading-edge effect, the one-dimensional framework can break down, although the details of the instabilities are still being investigated (Patterson *et al.* 2002; Daniels & Patterson 1997, 2001). Stability analyses of the one-dimensioinal steady-state solution obtained when ambient stratification is accounted for (Gill & Davey 1969; Bergholz 1978) suggest that stratification may exert a stabilizing influence on vertical plate convection.

Because of the ubiquity of stratified fluids in environmental and engineering flows, stratification effects are of fundamental interest in fluid mechanics and heat transfer research. Even in cases where the ambient fluid state is initially unstratified, a convective motion itself can lead to self-stratification and associated changes in the character of the motion, as in the case of enclosures with heated or cooled sidewalls (e.g. Hyun 1984; Lin & Armfield 2001). The extension of the one-dimensional natural convection framework to include ambient stratification is a relatively recent development. Park & Hyun (1998) and Park (2001) considered flow of a stratified fluid in the gap between two infinite parallel plates undergoing an impulsive (step) change in plate heat flux. Their solution was obtained as an eigenfunction expansion in which the dependence of the eigenvalues on Prandtl number and Rayleigh number revealed a partitioning of transient behaviour into oscillatory and monotonic approaches to steady-state conditions.

Shapiro & Fedorovich (2004*a*) considered the problem of convection in a stratified flow adjacent to a single infinite vertical plate. Analytical solutions were obtained by the method of Laplace transforms for a Prandtl number of unity for the cases of impulsive (step) change in plate perturbation temperature, sudden application of a plate heat flux, and for arbitrary temporal variations in plate perturbation temperature or plate heat flux. Vertical motion in a stably stratified fluid was found to be associated with a simple negative feedback mechanism: rising warm fluid cooled relative to the environment, whereas subsiding cool fluid warmed relative to

the environment. Because of this feedback, convective flows of a stably stratified fluid along an infinite vertical plate driven by an impulsive change of plate temperature or heat flux eventually approached a steady state, whereas the corresponding flows in an unstratified fluid did not. In a companion paper, Shapiro & Fedorovich (2004*b*) explored the Prandtl-number dependence of convection of a stably stratified fluid along a single vertical plate both numerically and analytically, through the use of a regular perturbation expansion and Laplace transforms. The developing boundary layers were found to be thicker, more vigorous, and more sensitive to the Prandtl number at smaller Prandtl numbers (< 1) than at larger Prandtl numbers (> 1). The gross temporal behaviour of the flow after the onset of convection was found to be of the oscillatory-decay type for Prandtl numbers near unity, and of the non-oscillatory-decay type for large Prandtl numbers.

In the present paper, analytical solutions are obtained for laminar natural convection flows of linearly stratified fluid along infinite vertical plates (§ 2) and circular cylinders (§ 3) undergoing temporally periodic surface-temperature variations. The plate and cylinder solutions are valid for arbitrary ambient stratification, forcing frequency and Prandtl number. However, these solutions apply only to the purely periodic regime, and do not describe the transient (start-up) stage of a flow started from rest. In order to study this start-up flow stage and verify that the analytical solutions provide the appropriate description of the terminal state of the convective flow started from rest, a numerical model is introduced (§ 4). Because of the close similarity in the behaviour of the plate and cylinder solutions in the periodic regime, only numerical results for the plate are considered (§ 5).

2. Theory for convection driven by temporally periodic variations in surface temperature of plates

The governing equations for one-dimensional (parallel) laminar natural convection in the Boussinesq approximation are discussed in detail in Shapiro & Fedorovich (2004*a*). Under the one-dimensional restriction, the Boussinesq form of mass conservation is satisfied identically, while the horizontal equations of motion reduce to statements that the horizontal components of the pressure gradient are zero (pressure is horizontally uniform). The dimensionless vertical equation of motion and thermodynamic energy equation (with or without a slight modification for pressure work) for a linearly stratified fluid reduce to

$$\frac{\partial W}{\partial \tau} = \theta + \frac{\partial^2 W}{\partial \xi^2}, \tag{1}$$

$$\frac{\partial \theta}{\partial \tau} = -W + \frac{1}{Pr}\frac{\partial^2 \theta}{\partial \xi^2}. \tag{2}$$

Here, ξ is the horizontal (plate-normal) coordinate, τ is time, θ is perturbation temperature (in the interest of brevity we will sometimes omit the word 'perturbation'), W is vertical velocity, and Pr is the Prandtl number ($\equiv \nu/\kappa$, where the kinematic viscosity ν and thermal diffusivity κ are considered to be constant). These non-dimensional variables (ξ, τ, θ, W) are related to their dimensional counterparts (x, t, T', w) by,

$$\xi \equiv x\frac{(g\gamma/T_r)^{1/4}}{\sqrt{\nu}}, \quad \tau \equiv t\sqrt{g\gamma/T_r}, \quad \theta \equiv \frac{T'}{T'_0}, \quad W \equiv \frac{w}{T'_0}\sqrt{\gamma T_r/g}, \tag{3}$$

where γ is the ambient stratification parameter [$\equiv \mathrm{d}T_\infty/\mathrm{d}z$ for Boussinesq flow of liquids or gases; $\equiv \mathrm{d}T_\infty/\mathrm{d}z + g/c_p$ for a perfect gas with pressure work term retained], z is height, $T_\infty(z)$ is a linearly varying ambient temperature, $T'(x,t) \equiv T(x,z,t) - T_\infty(z)$, T_0' is the amplitude of the temperature perturbation at the plate surface, and T_r is a constant reference temperature. The corresponding inviscid system (dimensional version of (1) and (2) with $\nu = \kappa = 0$) admits travelling waves of the form $w \propto \sin(kx - \sqrt{g\gamma/T_r}\,\tau)$, $T' \propto \cos(kx - \sqrt{g\gamma/T_r}\,\tau)$, and *en masse* temporal oscillations of the form $w \propto \sin(\sqrt{g\gamma/T_r}\,\tau)$, $T' \propto \cos(\sqrt{g\gamma/T_r}\,\tau)$. These inviscid solutions have a circular frequency equal to the Brunt–Väisälä (buoyancy) frequency $\sqrt{g\gamma/T_r}$ (Kundu & Cohen 2002). The non-dimensional value of this frequency (following (3)) is unity.

The plate is located at $\xi = 0$, and fluid fills the semi-infinite domain $\xi > 0$. The no-slip condition is imposed at the plate surface, $\mathrm{W}(0, \tau) = 0$. The perturbation temperature at the plate surface is a temporal oscillation with circular frequency ω and an amplitude of unity, $\theta(0, \tau) = \cos\omega\tau$. This fixed dimensionless amplitude is a consequence of the non-dimensionalization, and does not represent any loss of generality. Since the thermal forcing originates at the plate surface, and the medium is viscous, the disturbance is considered to vanish far from the plate, except for the case of resonance (imposed frequency equal to the natural frequency of the inviscid system, $\omega = 1$), where an extension of the disturbance to infinity is found to be unavoidable.

We seek solutions of (1) and (2) in the form of simple harmonic oscillations:

$$\theta = \mathrm{Re}[A(\xi)\,\exp(-\mathrm{i}\omega\tau)], \tag{4}$$

$$W = \mathrm{Re}[B(\xi)\,\exp(-\mathrm{i}\omega\tau)], \tag{5}$$

where, A and B are complex-valued functions, and, without loss of generality, ω is considered to be positive. Substitution of (4) and (5) into (1) and (2), yields two coupled ordinary differential equations (fourth-order system),

$$-\mathrm{i}\omega A = -B + \frac{1}{Pr}\frac{\mathrm{d}^2 A}{\mathrm{d}\xi^2}, \tag{6}$$

$$-\mathrm{i}\omega B = A + \frac{\mathrm{d}^2 B}{\mathrm{d}\xi^2}. \tag{7}$$

Applying the trial solutions $A = c\,\exp(\mu\xi)$ and $B = a\,\exp(\mu\xi)$ in (6) and (7) yields

$$c = -a(\mu^2 + \mathrm{i}\omega), \tag{8}$$

$$a = c(\mathrm{i}\omega + \mu^2/Pr). \tag{9}$$

Eliminating a and c from (8) and (9), we obtain a quartic equation for μ:

$$\mu^4 + \mathrm{i}\omega(Pr+1)\mu^2 - Pr(\omega^2 - 1) = 0. \tag{10}$$

Interpreted as a quadratic equation for μ^2, (10) can be solved as

$$\mu_1^2 = -\tfrac{1}{2}\mathrm{i}[\omega(Pr+1) + \sqrt{4Pr + \omega^2(Pr-1)^2}], \tag{11}$$

$$\mu_2^2 = -\tfrac{1}{2}\mathrm{i}[\omega(Pr+1) - \sqrt{4Pr + \omega^2(Pr-1)^2}], \tag{12}$$

Taking the square root of (11) and (12), and using $\sqrt{-i} = \pm(1-i)/\sqrt{2}$, we obtain the four roots,

$$\left.\begin{aligned} \mu_1 &= -\tfrac{1}{2}(1-\mathrm{i})\sqrt{\omega(Pr+1)+\sqrt{4Pr+\omega^2(Pr-1)^2}}, \\ \mu_2 &= -\tfrac{1}{2}(1-\mathrm{i})\sqrt{\omega(Pr+1)-\sqrt{4Pr+\omega^2(Pr-1)^2}}, \\ \mu_3 &= -\mu_1, \quad \mu_4 = -\mu_2. \end{aligned}\right\} \tag{13}$$

It is convenient to relate these roots to the (non-negative) constants k_+ and k_-, defined by

$$\left.\begin{aligned} k_+ &\equiv \tfrac{1}{2}\sqrt{\omega(Pr+1)+\sqrt{4Pr+\omega^2(Pr-1)^2}}, \\ k_- &\equiv \tfrac{1}{2}\sqrt{|\omega(Pr+1)-\sqrt{4Pr+\omega^2(Pr-1)^2}|}. \end{aligned}\right\} \tag{14}$$

Clearly, $\mu_1 = -(1-\mathrm{i})k_+$, while the form of μ_2 depends on the sign of $\Phi \equiv \omega(Pr+1) - \sqrt{4Pr+\omega^2(Pr-1)^2}$. If $\Phi > 0$, then $\mu_2 = -(1-\mathrm{i})k_-$, but if $\Phi < 0$, then $\mu_2 = -(1-\mathrm{i})\mathrm{i}k_- = -(1+\mathrm{i})k_-$. It is straightforward to show that, for any non-zero value of Pr, $\Phi > 0$ is equivalent to $\omega > 1$, while $\Phi < 0$ is equivalent to $\omega < 1$. Thus, we can rewrite (13) as

$$\mu_1 = -(1-\mathrm{i})k_+, \quad \mu_2 = -(1-S\mathrm{i})k_-, \quad \mu_3 = (1-\mathrm{i})k_+, \quad \mu_4 = (1-S\mathrm{i})k_-, \tag{15}$$

where S is the sign function of $\omega - 1$:

$$S = \mathrm{sgn}(\omega - 1) = \begin{cases} 1, & \omega > 1, \\ -1, & \omega < 1. \end{cases}$$

The special case of $\omega = 1$ will be considered at the end of this section.

To ensure that the disturbance vanishes far from the plate, the roots with positive real part (μ_3, μ_4) must be rejected. Application of the no-slip condition $B(0) = 0$ and the normalization condition $A(0) = 1$, and use of (11) and (12) for μ_1^2 and μ_2^2 then leads to the solution

$$\begin{aligned} \theta = {} & \frac{1}{2}\left[1 - \frac{\omega(1-Pr)}{\sqrt{4Pr+\omega^2(Pr-1)^2}}\right]\exp(-k_+\xi)\cos(k_+\xi - \omega\tau) \\ & + \frac{1}{2}\left[1 + \frac{\omega(1-Pr)}{\sqrt{4Pr+\omega^2(Pr-1)^2}}\right]\exp(-k_-\xi)\cos(Sk_-\xi - \omega\tau), \end{aligned} \tag{16}$$

$$\begin{aligned} W = {} & \frac{1}{\sqrt{4Pr+\omega^2(Pr-1)^2}}\exp(-k_+\xi)\sin(k_+\xi - \omega\tau) \\ & - \frac{1}{\sqrt{4Pr+\omega^2(Pr-1)^2}}\exp(-k_-\xi)\sin(Sk_-\xi - \omega\tau). \end{aligned} \tag{17}$$

For $\omega > 1$ ($S = 1$, $Sk_-\xi > 0$), the solution is composed of two waves that propagate away from the plate and decay exponentially with distance from the plate. Since the phases of these waves are $k_+\xi - \omega\tau$ and $Sk_-\xi - \omega\tau$, we see that k_+ and k_- can be interpreted as wavenumbers. Since $k_+ > k_- > 0$, the k_- wave has a larger wavelength ($2\pi/k_-$), greater phase speed (ω/k_-) and smaller attenuation factor $\exp(-k_-\xi)$ (larger e-folding penetration distance $1/k_-$) than the k_+ wave. These wavenumbers, which appear in the solution of the plate problem and the upcoming cylinder problem, are plotted as a function of Pr and ω (from (14)) in figure 1.

For $\omega < 1 (S = -1, Sk_-\xi < 0)$, the solution is again composed of a k_+ and k_- wave, each of which decays exponentially with distance from the plate, with the k_- wave

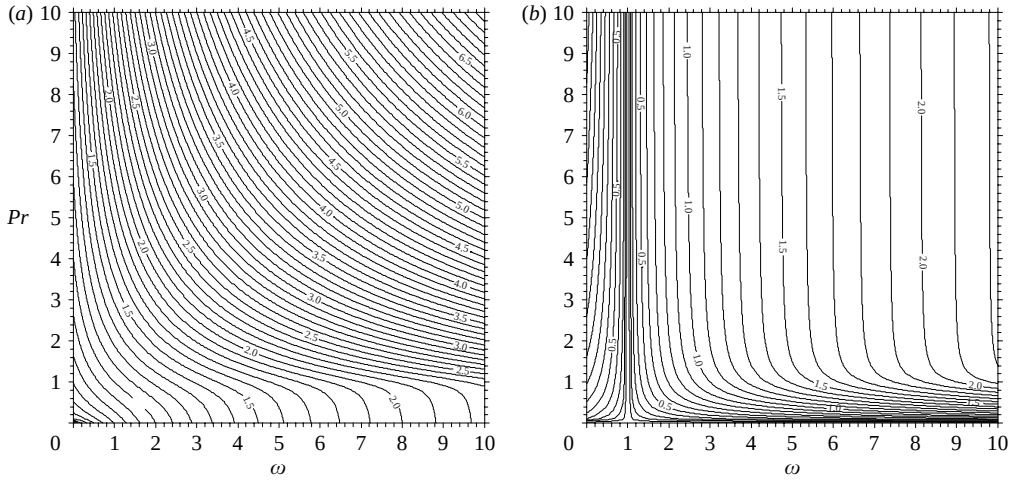

FIGURE 1. Wavenumber as a function of Pr and ω: (*a*) k_+ and (*b*) k_-, as determined from (14).

having a greater wavelength, greater phase speed and greater penetration distance than the k_+ wave. However, in this case, while the k_+ wave still propagates away from the plate, the k_- wave propagates toward the plate. It can be shown that for both $\omega < 1$ and $\omega > 1$, the k_+ and k_- waves are each associated with positive group velocities, that is, energy propagating away from the plate.

In the special case $\omega = 1$, the roots μ of (10) are $(1 - \mathrm{i})\sqrt{(Pr+1)/2}$, $-(1-\mathrm{i})\sqrt{(Pr+1)/2}$ and a double root 0. The general solution for A and B is a linear combination of (i) the two exponential terms associated with these first two roots, (ii) a constant term, and (iii) a term linear in ξ. It is clear that no particularization of the general solution will allow it to satisfy all of the originally stated boundary conditions. We interpet this as a case of resonance (forcing frequency equal to the buoyancy frequency – the natural frequency of the inviscid system), and suggest that the appropriate condition to relax is the condition that the disturbance vanishes at infinity. In its place, we require that the disturbance be bounded at infinity. This finiteness condition requires us to reject the linear term and the exponential term associated with the root with positive real part. The solutions satisfying the remaining (plate) boundary conditions are then found to be

$$\theta = \frac{\cos\tau}{1+Pr} + \frac{Pr}{1+Pr}\exp[-\sqrt{(Pr+1)/2}\xi]\cos[\sqrt{(Pr+1)/2}\xi - \tau] \quad \omega = 1, \quad (18)$$

$$W = \frac{\sin\tau}{1+Pr} + \frac{1}{1+Pr}\exp[-\sqrt{(Pr+1)/2}\xi]\sin[\sqrt{(Pr+1)/2}\xi - \tau] \quad \omega = 1. \quad (19)$$

Thus, the resonance solution is comprised of an outward-propagating spatially decaying wave and an *en masse* inviscid-like temporal oscillation.

3. Theory for convection driven by temporally periodic variations in surface temperature of cylinders

Next, consider convection along infinite vertical cylinders with temporally periodic variations in surface temperature. In cylindrical polar coordinates, the governing

equations become

$$\frac{\partial W}{\partial \tau} = \theta + \left(\frac{\partial^2}{\partial R^2} + \frac{1}{R}\frac{\partial}{\partial R}\right) W, \tag{20}$$

$$\frac{\partial \theta}{\partial \tau} = -W + \frac{1}{Pr}\left(\frac{\partial^2}{\partial R^2} + \frac{1}{R}\frac{\partial}{\partial R}\right)\theta. \tag{21}$$

Here, we have adopted the same non-dimensionalization as in the plate problem (namely, (3)), but with the spatial coordinate being the non-dimensional radial coordinate R, which is related to the dimensional radial coordinate r by

$$R \equiv r\frac{(g\gamma/T_r)^{1/4}}{\sqrt{\nu}}. \tag{22}$$

Similarly, the non-dimensional cylinder radius R_c is related to the dimensional cylinder radius r_c by

$$R_c \equiv r_c\frac{(g\gamma/T_r)^{1/4}}{\sqrt{\nu}}. \tag{23}$$

We again seek solutions in the form of simple harmonic oscillations,

$$\theta = \mathrm{Re}[A(R)\exp(-\mathrm{i}\omega\tau)], \tag{24}$$

$$W = \mathrm{Re}[B(R)\exp(-\mathrm{i}\omega\tau)]. \tag{25}$$

Substitution of (24) and (25) into (20) and (21) yields the differential equations,

$$-\mathrm{i}\omega B = A + \left(\frac{\mathrm{d}^2}{\mathrm{d}R^2} + \frac{1}{R}\frac{\mathrm{d}}{\mathrm{d}R}\right) B, \tag{26}$$

$$-\mathrm{i}\omega A = -B + \frac{1}{Pr}\left(\frac{\mathrm{d}^2}{\mathrm{d}R^2} + \frac{1}{R}\frac{\mathrm{d}}{\mathrm{d}R}\right) A. \tag{27}$$

Applying trial solutions of the form $A = cZ_0(\mathrm{i}\mu R)$, $B = aZ_0(\mathrm{i}\mu R)$ in (26) and (27), where μ is an as yet undetermined parameter and Z_0 is any Bessel function of order zero (any solution of $(\mathrm{d}^2/\mathrm{d}R^2 + 1/R\mathrm{d}/\mathrm{d}R - \mu^2)Z_0(\mathrm{i}\mu R) = 0$), we obtain the compatability conditions,

$$c = -(\mathrm{i}\,\omega + \mu^2)\,a, \tag{28}$$

$$a = (\mathrm{i}\,\omega + \mu^2/Pr)\,c. \tag{29}$$

Since (28) and (29) are identical to (8) and (9) for the plate problem, the previous expressions (10)–(15) for μ, k_+, k_-, including the special considerations for $\omega \lesssim 1$, also apply to the cylinder problem. In view of these results, A and B can be expressed as linear combinations of $H_0^1[(1+\mathrm{i})k_+R]$, $H_0^1[(S+\mathrm{i})k_-R]$, $H_0^2[(1+\mathrm{i})k_+R]$, and $H_0^2[(S+\mathrm{i})k_-R]$, where H_0^1 and H_0^2 are Hankel functions of the first and second kind (Bessel functions of the third kind). However, since the imaginary parts of the arguments of these functions are positive, and only Hankel functions of the first kind vanish when their arguments become infinite with positive imaginary part (Jahnke & Emde 1945), we must reject the $H_0^2[(1+\mathrm{i})k_+R]$ and $H_0^2[(S+\mathrm{i})k_-R]$ functions to ensure that A and B vanish far from the cylinder. Application of the no-slip condition $B(R_c) = 0$ and the normalization condition $A(R_c) = 1$, and use of (11) and (12) for μ_1^2

and μ_2^2 then leads to the determination of A and B as

$$A = \frac{1}{2}\left[1 + \frac{\omega(Pr-1)}{\sqrt{4Pr+\omega^2(Pr-1)^2}}\right]\frac{H_0^1[(1+\mathrm{i})k_+R]}{H_0^1[(1+\mathrm{i})k_+R_c]} + \frac{1}{2}\left[1 - \frac{\omega(Pr-1)}{\sqrt{4Pr+\omega^2(Pr-1)^2}}\right]\frac{H_0^1[(S+\mathrm{i})k_-R]}{H_0^1[(S+\mathrm{i})k_-R_c]}, \tag{30}$$

$$B = \frac{\mathrm{i}}{\sqrt{4Pr+\omega^2(Pr-1)^2}}\left[\frac{H_0^1[(S+\mathrm{i})k_-R]}{H_0^1[(S+\mathrm{i})k_-R_c]} - \frac{H_0^1[(1+\mathrm{i})k_+R]}{H_0^1[(1+\mathrm{i})k_+R_c]}\right]. \tag{31}$$

To help identify the real and imaginary parts of (30) and (31), we express these Hankel functions in terms of Kelvin functions (Abramowitz & Stegun 1964, hereinafter referred to as AS). The arguments of these Hankel functions can be put in the form of either $(1+\mathrm{i})x$ or $(-1+\mathrm{i})x$, where x is a real number. Writing $(-1+\mathrm{i})x$ as $x\sqrt{2}\exp(3\pi\mathrm{i}/4)$, and applying (9.9.2) of AS, yields

$$H_0^1[(-1+\mathrm{i})x] = \frac{2}{\pi}[kei_0(x\sqrt{2}) - \mathrm{i}ker_0(x\sqrt{2})], \tag{32}$$

where ker_0 and kei_0 are Kelvin functions of order zero. Since $ker_0(y) = N_0(y)\cos\phi_0(y)$ and $kei_0(y) = N_0(y)\sin\phi_0(y)$, where $N_0(y) \equiv \sqrt{ker_0^2(y) + kei_0^2(y)}$ is the modulus and $\phi_0(y) = \arctan[kei_0(y)/ker_0(y)]$ the phase ((9.10.18) and (9.10.19) of AS), (32) becomes

$$H_0^1[(-1+\mathrm{i})x] = -\mathrm{i}\frac{2}{\pi}N_0(x\sqrt{2})\exp[\mathrm{i}\phi_0(x\sqrt{2})]. \tag{33}$$

Writing $(1+\mathrm{i})x$ as $x\sqrt{2}\exp(\pi\mathrm{i}/4)$ and using (9.1.40) of AS yields $H_0^1[(1+\mathrm{i})x] = \overline{H_0^2[x\sqrt{2}\exp(-\pi\mathrm{i}/4)]}$ where the overbar denotes the complex conjugate. Applying (9.9.2) of AS to this latter term, and rearranging, we obtain

$$H_0^1[(1+\mathrm{i})x] = -\frac{2}{\pi}[kei_0(x\sqrt{2}) + \mathrm{i}ker_0(x\sqrt{2})]. \tag{34}$$

In terms of the modulus and phase functions, (34) becomes

$$H_0^1[(1+\mathrm{i})x] = -\mathrm{i}\frac{2}{\pi}N_0(x\sqrt{2})\exp[-\mathrm{i}\phi_0(x\sqrt{2})]. \tag{35}$$

Equations (33) and (35) can be combined as

$$H_0^1[(S+\mathrm{i})x] = -\mathrm{i}\frac{2}{\pi}N_0(x\sqrt{2})\exp[-\mathrm{i}S\phi_0(x\sqrt{2})]. \tag{36}$$

Collecting results, we obtain the temperature and vertical velocity fields as

$$\theta = \frac{1}{2}\left[1 + \frac{\omega(Pr-1)}{\sqrt{4Pr+\omega^2(Pr-1)^2}}\right]\frac{N_0(k_+R\sqrt{2})}{N_0(k_+R_c\sqrt{2})} \times \cos[-\phi_0(k_+R\sqrt{2}) - \omega\tau + \phi_0(k_+R_c\sqrt{2})] + \frac{1}{2}\left[1 - \frac{\omega(Pr-1)}{\sqrt{4Pr+\omega^2(Pr-1)^2}}\right]\frac{N_0(k_-R\sqrt{2})}{N_0(k_-R_c\sqrt{2})} \times \cos[-S\phi_0(k_-R\sqrt{2}) - \omega\tau + S\phi_0(k_-R_c\sqrt{2})], \tag{37}$$

$$W = \frac{1}{\sqrt{4Pr+\omega^2(Pr-1)^2}} \frac{N_0(k_+R\sqrt{2})}{N_0(k_+R_c\sqrt{2})} \sin[-\phi_0(k_+R\sqrt{2})-\omega\tau+\phi_0(k_+R_c\sqrt{2})]$$
$$- \frac{1}{\sqrt{4Pr+\omega^2(Pr-1)^2}} \frac{N_0(k_-R\sqrt{2})}{N_0(k_-R_c\sqrt{2})} \sin[-S\phi_0(k_-R\sqrt{2})-\omega\tau+S\phi_0(k_-R_c\sqrt{2})]. \tag{38}$$

The wave characteristics in (37) and (38) are very similar to those in the plate problem. Since ϕ_0 is negative for all real values of its argument (see figures 9.11 and (9.10.26) of AS), (37) and (38) indicate that the k_+ wave propagates away from the cylinder while the k_- wave propagates away from the cylinder if $\omega > 1 (S = 1)$, but toward the cylinder if $\omega < 1 (S = -1)$. Moreover, since the asymptotic (large argument) form of ϕ_0 is $\phi_0(x) \sim -x/\sqrt{2}$, and this linear dependence of ϕ_0 on its argument is a good approximation throughout much of the range of its argument (figure 9.11 of AS), the phase of the k_+ wave, $-\phi_0(k_+R\sqrt{2})-\omega\tau+\phi_0(k_+R_c\sqrt{2})$ is approximately $k_+(R-R_c)-\omega\tau$, while the phase of the k_- wave, $-S\phi_0(k_-R\sqrt{2})-\omega\tau+S\phi_0(k_-R_c\sqrt{2})$ is approximately $Sk_-(R-R_c)-\omega\tau$. These approximate phases are the exact phases for the k_+ and k_- waves in the plate problem, (16) and (17), with distance from the plate ξ written in place of distance from the cylinder $R-R_c$.

Equations (37) and (38) apply to cylinders of any size, including wires (very small cylinders). They can be evaluated using standard ascending series and asymptotic formulae for Kelvin functions. However, the forms of (37) and (38) simplify greatly if we restrict attention to large cylinder radii. Using the first term asymptotic formulae $N_0(x) \sim \sqrt{\pi/(2x)}\exp(-x/\sqrt{2})$, and $\phi_0(x) \sim -x/\sqrt{2}$ valid for $x \to \infty$ ((9.10.24) and (9.10.26) of AS), (37) and (38) can be approximated well as

$$\theta \sim \frac{1}{2}\left[1+\frac{\omega(Pr-1)}{\sqrt{4Pr+\omega^2(Pr-1)^2}}\right]\sqrt{\frac{R_c}{R}}\exp[-k_+(R-R_c)]\cos[k_+(R-R_c)-\omega\tau]$$
$$+\frac{1}{2}\left[1-\frac{\omega(Pr-1)}{\sqrt{4Pr+\omega^2(Pr-1)^2}}\right]\sqrt{\frac{R_c}{R}}\exp[-k_-(R-R_c)]\cos[Sk_-(R-R_c)-\omega\tau],$$
$$\text{large } k_+R_c, k_-R_c, \tag{39}$$
$$W \sim \frac{1}{\sqrt{4Pr+\omega^2(Pr-1)^2}}\sqrt{\frac{R_c}{R}}\exp[-k_+(R-R_c)]\sin[k_+(R-R_c)-\omega\tau]$$
$$-\frac{1}{\sqrt{4Pr+\omega^2(Pr-1)^2}}\sqrt{\frac{R_c}{R}}\exp[-k_-(R-R_c)]\sin[Sk_-(R-R_c)-\omega\tau],$$
$$\text{large } k_+R_c, k_-R_c. \tag{40}$$

For locations close enough to the cylinder that the distance $\Xi \equiv R-R_c$ is a small fraction of the cylinder radius ($\Xi/R_c \ll 1$), $R/R_c = 1+\Xi/R_c \approx 1$, (39) and (40) can be further approximated as

$$\theta \sim \frac{1}{2}\left[1+\frac{\omega(Pr-1)}{\sqrt{4Pr+\omega^2(Pr-1)^2}}\right]\exp(-k_+\Xi)\cos(k_+\Xi-\omega t)$$
$$+\frac{1}{2}\left[1-\frac{\omega(Pr-1)}{\sqrt{4Pr+\omega^2(Pr-1)^2}}\right]\exp(-k_-\Xi)\cos(Sk_-\Xi-\omega t),$$
$$\text{large } k_+R_c, k_-R_c; \frac{\Xi}{R_c} \ll 1. \tag{41}$$

$$W \sim \frac{1}{\sqrt{4Pr+\omega^2(Pr-1)^2}}\exp(-k_+\Xi)\sin(k_+\Xi-\omega t) - \frac{1}{\sqrt{4Pr+\omega^2(Pr-1)^2}}\exp(-k_-\Xi)\sin(Sk_-\Xi-\omega t),$$

$$\text{large } k_+R_c, k_-R_c; \frac{\Xi}{R_c} \ll 1. \quad (42)$$

The large radius/small distance solutions (41) and (42) are identical to (16) and (17), with distance from the cylinder Ξ in place of distance from the plate ξ, indicating that for a cylinder of large radius, the flow behaves locally (near the cylinder) as if it were near a plate. However, if for large cylinders we consider locations not close to the cylinder (in the sense that Ξ/R_c is not much less than 1), we must use (39) and (40), which is equivalent to the flat-plate solution (16) and (17) reduced by a factor of $\sqrt{R_c/R}$.

Finally, we consider the special case $\omega = 1$. Here, the general solution for A and B is a linear combination of (i) $H_0^1[(1+\mathrm{i})\sqrt{(Pr+1)/2}R]$ and $H_0^2[(1+\mathrm{i})\sqrt{(Pr+1)/2}R]$, (ii) a constant term, and (iii) a $\ln R$ term. To ensure the solution is bounded at infinity, we reject the second of these Hankel functions and the $\ln R$ term. The solutions satisfying the remaining (cylinder) boundary conditions are then found to be

$$\theta = \frac{\cos\tau}{1+Pr} + \frac{Pr}{1+Pr}\frac{N_0(k_+R\sqrt{2})}{N_0(k_+R_c\sqrt{2})}\cos[-\phi_0(k_+R\sqrt{2}) - \tau + \phi_0(k_+R_c\sqrt{2})], \quad \omega = 1, \quad (43)$$

$$W = \frac{\sin\tau}{1+Pr} + \frac{1}{1+Pr}\frac{N_0(k_+R\sqrt{2})}{N_0(k_+R_c\sqrt{2})}\sin[-\phi_0(k_+R\sqrt{2}) - \tau + \phi_0(k_+R_c\sqrt{2})], \quad \omega = 1, \quad (44)$$

Again, we find that the resonance solution is comprised of an outward-propagating spatially decaying wave and an *en masse* temporal oscillation.

4. Numerical model

A numerical model is applied to the initial-value problem in which a resting fluid is suddenly subjected to a plate perturbation temperature in the form of a periodic (cosine) wave:

$$\left.\begin{aligned} &\theta(x,0) = 0, \qquad \theta(0,t) = \begin{cases} 0, & t = 0, \\ \cos\omega t, & t > 0, \end{cases} \\ &W(x,0) = 0, \qquad W(0,t) = 0. \end{aligned}\right\} \quad (45)$$

These numerical results depict the transient (start-up) stage of the flow, as will be shown below, and confirm that the analytical solutions of § 2 provide the appropriate description of a later-stage periodic regime.

The numerical model used in this study was originally designed to support work on instabilities and transition to turbulent regimes of natural convection in a stably stratified fluid. However, the model can also be used to study laminar (one-dimensional) natural convection along a vertical plate in cases where flow parameters are consistent with maintenance of a laminar flow regime. The model solves the three-dimensional Boussinesq equations of motion, thermodynamic energy and mass

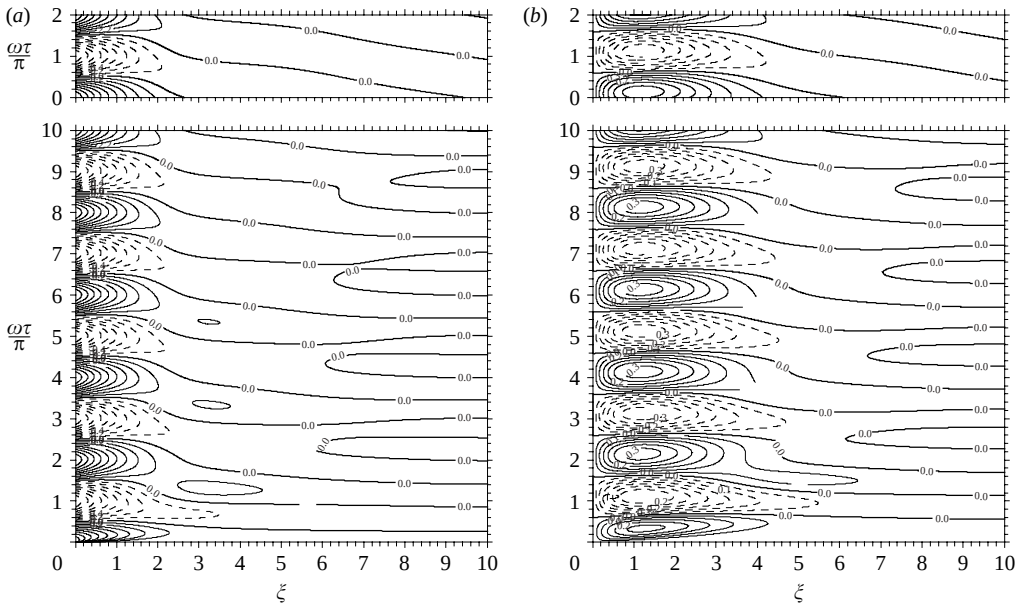

FIGURE 2. Contour plots of (*a*) θ and (*b*) W as functions of ξ and τ from the numerically simulated case of $Pr = 1$ and $\omega = 0.5$ for the first five periods of surface thermal oscillation. At the top of (*a*) and (*b*) is a contour plot of the corresponding analytical solution for one period of oscillation. Positive (and zero) contours are solid; negative contours are dashed.

conservation on a staggered Cartesian (x, y, z) grid stretched along the plate-normal (x) direction. The three velocity components and the perturbation temperature field are treated as prognostic variables, while the perturbation pressure field is diagnosed from the elliptic equation that results from taking the three-dimensional divergence of the equations of motion and enforcing the Boussinesq form of the mass conservation equation. The model is patterned on the works of Fedorovich, Nieuwstadt & Kaiser (2001) and Nieuwstadt (1990), and is summarized in Shapiro & Fedorovich (2004*b*). This latter reference also describes a validation test of the computer code.

The values of the plate perturbation temperature and the physical parameters of the problem (T_r, γ, ν, κ) used for the numerical simulations reported herein were such that flow instabilities did not develop. At the computational boundary far from the plate (large x), a zero gradient condition is imposed. Periodic boundary conditions were imposed for all variables on the four x–y and x–z computational boundaries of the domain. The output velocity and temperature perturbation fields were averaged over the (y, z)-planes. However, as long as the flow remained laminar (which was the case for all results reported herein), variations of these quantities in the (y, z)-planes were negligible. Although the model itself is dimensional, the output is made non-dimensional following (3) so as to facilitate comparisons with the analytical results.

5. Examples of convection along a vertical plate

We first consider cases of various forcing frequencies with $Pr = 1$. Figure 2 depicts contour plots of θ and W for $\omega = 0.5$, a case where the forcing frequency is less than the natural frequency of the inviscid system. In this figure, the numerical solution for the first five periods of thermal oscillation is presented, together with the corresponding

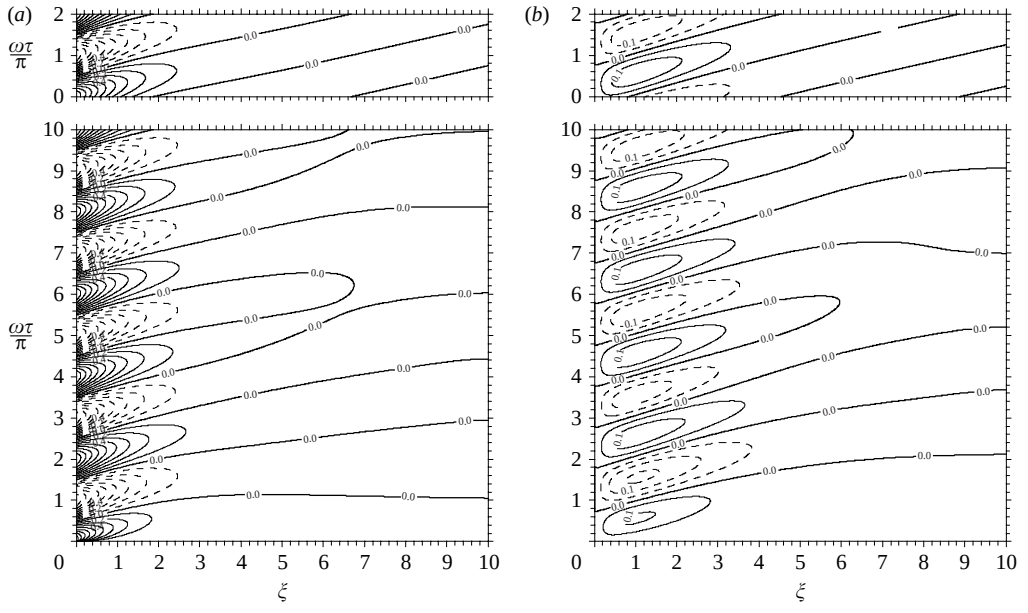

FIGURE 3. As in figure 2, but for $Pr = 1$ and $\omega = 2$.

analytical solution for the periodic regime. In the region of the main disturbance, near the plate (say, $\xi < 3$), the numerical solution approaches the analytical solution within just a few oscillation periods. Far from the plate, where the disturbance becomes weak, the negative slopes of the zero contours in the analytical solutions for θ and W indicate an inward-propagating wave. Such negative slopes begin to emerge in the numerical solution at the later times in the figure (and become even more evident at times later than those depicted here.)

Figure 3 presents the numerical and analytical contour plots for $Pr = 1$ and $\omega = 2$, a case where the forcing frequency is greater than the natural frequency. We again see a rapid approach of the numerical solution to the analytical solution in the region of the main disturbance, near the plate, with a slower approach to the analytical solution in the regions further from the plate. In this case, the positive slopes of the zero contours for θ and W far from the plate indicate an outward-propagating wave.

The case with $Pr = 1$ and forcing frequency equal to the natural frequency, $\omega = 1$ (the resonance case), is depicted in figures 4–6. The contour plots of θ and W presented in figures 4 and 5 show that the numerical solution approaches the analytical solution (top of figure 5) at large ξ relatively slowly. The periodic regime is characterized by *en masse* temporal oscillations of the entire fluid, with the exception of the boundary layer in the immediate vicinity of the plate whose structure is dominated by the no-slip condition. The slow convergence of the numerical solution to the analytical solution at large ξ is highlighted in figure 6.

Finally, we present contour plots of the analytical solutions for $Pr = 0.71$, 1 and 7.1 for the case of a small forcing frequency, $\omega = 0.1$ (figure 7), and a large forcing frequency $\omega = 10$ (figure 8). The Prandtl numbers 0.71 and 7.1 are the values for dry air at a temperature of 30 °C at atmospheric pressure and pure water at a temperature of 20 °C at atmospheric pressure, respectively (Kundu & Cohen 2002). In figures 7 and 8, we see that both the thickness of the thermal boundary layer and the intensity of the vertical motion increase with decreasing Prandtl number. This behaviour is

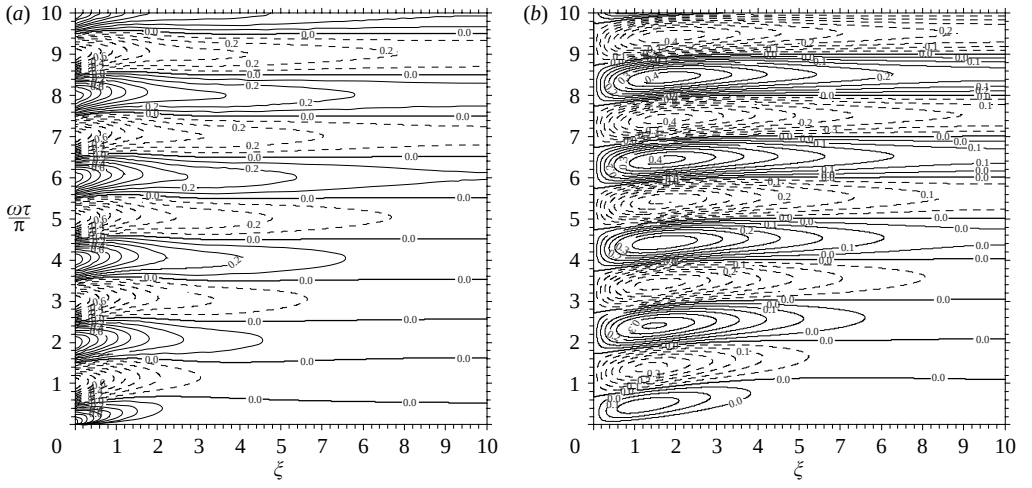

FIGURE 4. Contour plots of (*a*) θ and (*b*) W as functions of ξ and τ from the numerically simulated case of $Pr = 1$ and $\omega = 1$ for the first five periods of surface thermal oscillation. Positive (and zero) contours are solid; negative contours are dashed.

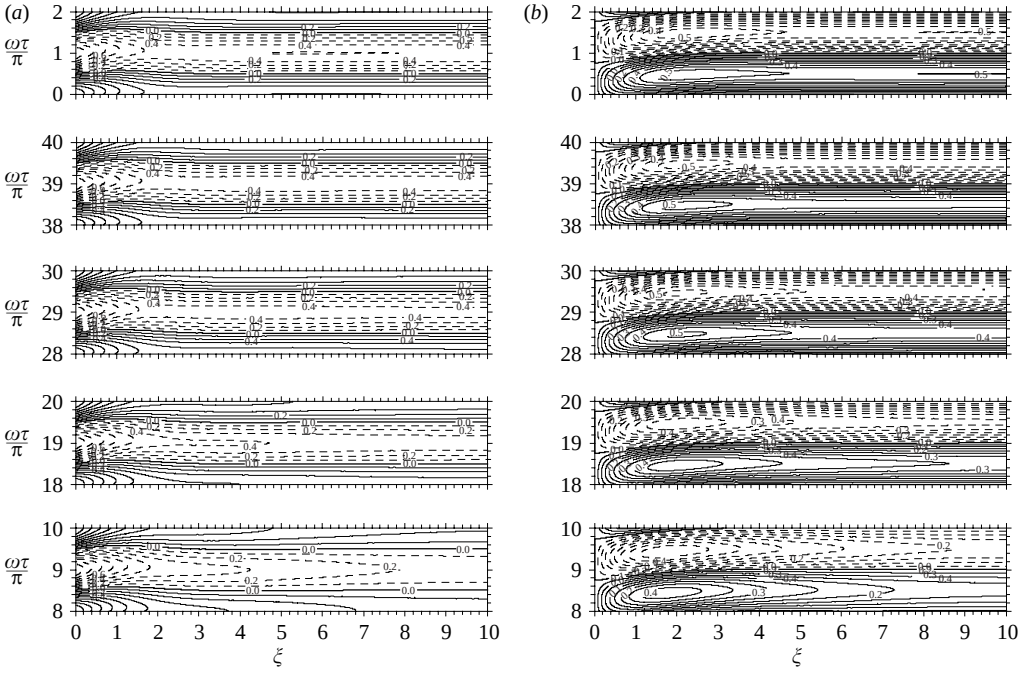

FIGURE 5. As in figure 4, but for selected later time periods. At the top of (*a*) and (*b*) is a contour plot of the corresponding analytical solution for one period of oscillation.

qualitatively similar to what is found in unsteady convective flows induced by an impulsive change in the surface temperature of a vertical plate immersed in a stably stratified fluid (Shapiro & Fedorovich 2004*b*) and in the corresponding steady-state flows (e.g. Gill 1966; Bergholz 1978). The generally negative slopes of the zero contours of θ and W far from the plate in the $\omega = 0.1$ solutions (figure 7) indicate

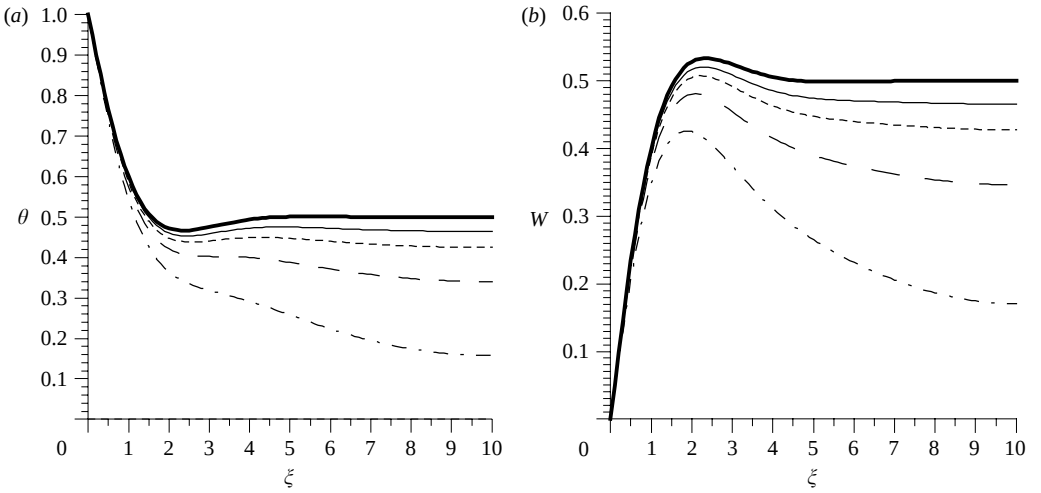

FIGURE 6. Numerical solutions for (*a*) θ and (*b*) W as functions of ξ for $Pr = 1$ and $\omega = 1$ at different 2π intervals of time. Each W curve is a quarter-period ahead of the corresponding θ curve. The θ curves correspond to $\tau/\pi = 8$ (dashed and dotted line), $\tau/\pi = 18$ (long-dash line), $\tau/\pi = 28$ (short-dash line), and $\tau/\pi = 38$ (solid line). Bold lines show periodic analytical solutions for θ at $\tau/\pi = 2n$ and W at $\tau/\pi = 2n + 1/2$.

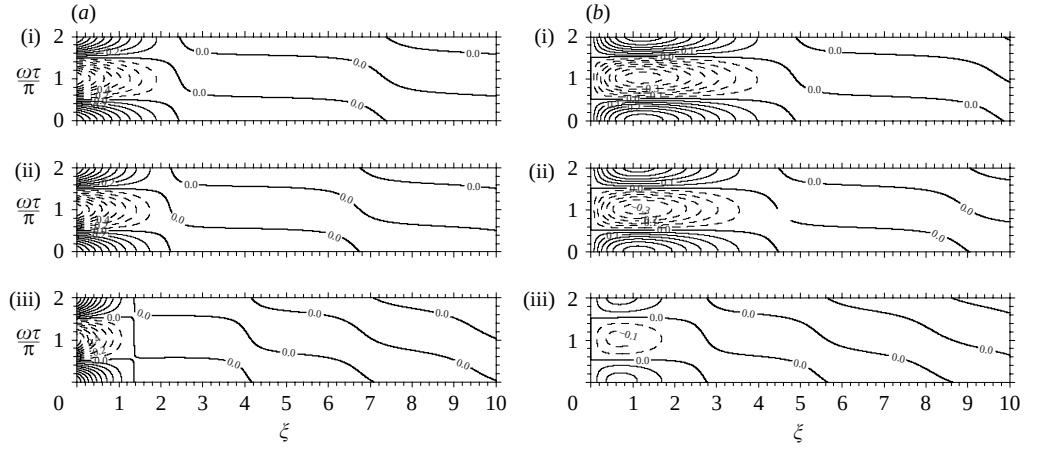

FIGURE 7. Analytical solutions for (*a*) θ and (*b*) W as functions of ξ and τ for $\omega = 0.1$ (i) $Pr = 0.71$; (ii) $Pr = 1$; (iii) $Pr = 7.1$. Positive (and zero) contours are solid; negative contours are dashed.

an inward-propagating wave. In the case $\omega = 10$ (figure 8) the positive slopes of the zero contours of θ and W far from the plate indicate an outward-propagating wave. We also see that in the lower panels of figures 8(*a*) and (*b*) (i.e. for $Pr = 7.1$), the zero contours for θ are steeper and packed closer together near the plate than far from the plate, while the slopes and spacing of the zero contours for W are relatively insensitive to distance from the plate. To explain this behaviour, we first note that for $Pr = 7.1$ and $\omega = 10$, the k_+ wavenumber is almost three times larger than the k_- wavenumber (figure 1), hence the phase speed for the k_+ wave is only about 30% of the speed of the k_- wave (so the slope of the zero contours in the

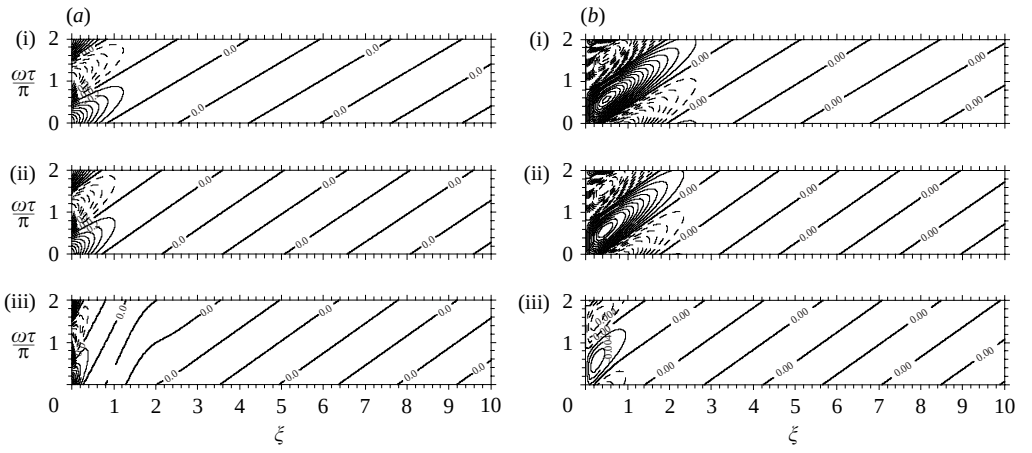

FIGURE 8. As in figure 7 but for $\omega = 10$.

(ξ, τ)-plane should be steeper for the k_+ wave than the k_- wave). However, the extent to which these wave characteristics become manifest depends, in part, on the relative magnitudes of the coefficients in front of the k_+ and k_- wave terms in (16) and (17). It can readily be shown that for W, the numerical factors in front of the k_+ and k_- wave terms are equal, but that for θ, the numerical factor in front of the k_+ wave term is approximately 1000 times larger than the factor in front of the k_- wave term. Accordingly, the k_+ wave characteristics will be much more apparent in the θ field than in the W field, at least near the plate (since the penetration distance of the k_- wave is greater than that of the k_+ wave, the k_- wave will eventually dominate far from the plate in both θ and W solutions).

6. Summary

Analytical solutions of the viscous Boussinesq equations of motion and thermodynamic energy are presented for the laminar natural convection flow of a linearly stratified fluid along infinite vertical plates and circular cylinders with temporally periodic surface-temperature variations. Although our focus has been on the fundamental behaviour of a class of simple natural convection flows, the solutions may be of practical interest to those concerned with heat transfer problems in reciprocating flows; oscillatory flows in which the amplitude of the oscillatory velocity is greater than that of the time-mean velocity (see review article by Zhao & Cheng 1998).

Our solutions are considered to be valid for the purely periodic regime, that is, for times long enough after start-up that transient effects have dissipated. The behaviour of the solutions are qualitatively similar for plates and cylinders, and are crucially dependent on the value of the frequency of the imposed thermal oscillation. For forcing frequencies greater than the natural frequency of the inviscid system (buoyancy frequency), the disturbance consists of two outward-propagating waves. For forcing frequencies less than the natural frequency, the disturbance is comprised of an outward-propagating wave and in inward-propagating wave, a scenario in which the conventional radiation condition is not appropriate. In both cases, the waves decrease exponentially with distance from the surface. The case where the forcing frequency is equal to the natural frequency results in *en masse* temporal oscillations of

the fluid. In this resonance case, the disturbance extends an infinite distance from the surface. Within this general behavioural framework, there is additional complexity associated with the values of the Prandtl number. In particular, the values of the Prandtl number and forcing frequency together determine the extent to which one or other of the two waves dominates the solution for θ (but not W) near the plate. The analytical results were complemented with numerical simulations initialized from a state of rest. The numerical results suggest that the analytical solutions do provide appropriate descriptions of impulsively started oscillatory convection after sufficiently long periods of time have elapsed.

REFERENCES

Abramowitz, M. & Stegun, I. A. 1964 *Handbook of Mathematical Functions with Formulas, Graphs, and Mathematical Tables*. National Bureau of Standards, Washington, DC.

Armfield, S. W. & Patterson, J. C. 1992 Wave properties of natural convection boundary layers. *J. Fluid Mech.* **239**, 195–211.

Barletta, A. & di Schio, E. R. 2004 Mixed convection flow in a vertical circular duct with time-periodic boundary conditions: steady-periodic regime. *Intl J. Heat Mass Transfer* **47**, 3187–3195.

Bergholz, R. F. 1978 Instability of steady natural convection in a vertical fluid layer. *J. Fluid Mech.* **84**, 743–768.

Daniels, P. G. & Patterson, J. C. 1997 On the long-wave instability of natural-convection boundary layers. *J. Fluid Mech.* **335**, 57–73.

Daniels, P. G. & Patterson, J. C. 2001 On the short-wave instability of natural convection boundary layers. *Proc. R. Soc. Lond.* A **457**, 519–538.

Das, U. N., Deka, R. K. & Soundalgekar, V. M. 1999 Transient free convection flow past an infinite vertical plate with periodic temperature variation. *J. Heat Transfer* **121**, 1091–1094.

Fedorovich, E., Nieuwstadt, F. T. M. & Kaiser, R. 2001 Numerical and laboratory study of a horizontally evolving convective boundary layer. Part I: Transition regimes and development of the mixed layer. *J. Atmos. Sci.* **58**, 70–86.

Gebhart, B., Jaluria, Y., Mahajan, R. L. & Sammakia, B. 1988 *Buoyancy-Induced Flows and Transport*. Hemisphere.

Gill, A. E. 1966 The boundary layer regime for convection in a rectangular cavity. *J. Fluid Mech.* **26**, 515–536.

Gill, A. E. & Davey, A. 1969 Instabilities of a buoyancy-driven system. *J. Fluid Mech.* **35,** 775–798.

Goldstein, R. J. & Briggs, D. G. 1964 Transient free convection about vertical plates and circular cylinders. *Trans. ASME: J. Heat Transfer* **86**, 490–500.

Hyun, J. M. 1984 Transient process of thermally stratifying an initially homogeneous fluid in an enclosure. *Intl J. Heat Mass Transfer* **27**, 1936–1938.

Illingworth, C. R. 1950 Unsteady laminar flow of a gas near an infinite flat plate. *Proc. Camb. Phil. Soc.* **46**, 603–613.

Jahnke, E. & Emde, F. 1945 *Tables of Functions with Formulae and Curves*. Dover.

Kundu, P. K. & Cohen, I. M. 2002 *Fluid Mechanics*. Academic.

Lin, W. X. & Armfield, S. W. 2001 Natural convection cooling of rectangular and cylindrical containers. *Intl J. Heat Fluid Flow* **22**, 72–81.

Menold, E. R. & Yang, K.-T. 1962 Asymptotic solutions for unsteady laminar free convection on a vertical plate. *Trans. ASME: J. Appl. Mech.* **29**, 124–126.

Nieuwstadt, F. T. M. 1990 Direct and large-eddy simulation of free convection. *Proc. Ninth Intl Heat Transfer Conf. Jerusalem, Israel*, pp. 37–47.

Park, J. S. 2001 Transient buoyant flows of a stratified fluid in a vertical channel. *KSME Intl J.* **15**, 656–664.

Park, J. S. & Hyun, J. M. 1998 Transient behaviour of vertical buoyancy layer in a stratified fluid. *Intl J. Heat Mass Transfer* **41**, 4393–4397.

Patterson, J. C., Graham, T., Schöpf, W. & Armfield, S. W. 2002 Boundary layer development on a semi-infinite suddenly heated vertical plate. *J. Fluid Mech.* **453**, 39–55.

Schetz, J. A. & Eichhorn, R. 1962 Unsteady natural convection in the vicinity of a doubly-infinite vertical plate. *Trans. ASME: J. Heat Transfer* **84**, 334–338.

Schladow, S. G. 1990 Oscillatory motion in a side-heated cavity. *J. Fluid Mech.* **213**, 589–610.

Schöpf, W. & Patterson, J. C. 1995 Natural-convection in a side-heated cavity – visualization of the initial flow features. *J. Fluid Mech.* **295**, 357–379.

Shapiro, A. & Fedorovich, E. 2004*a* Unsteady convectively driven flow along a vertical plate immersed in a stably stratified fluid. *J. Fluid Mech.* **498**, 333–352.

Shapiro, A. & Fedorovich, E. 2004*b* Prandtl number dependence of unsteady natural convection along a vertical plate in a stably stratified fluid. *Intl J. Heat Mass Transfer* **47**, 4911–4927.

Siegel, R. 1958 Transient free convection from a vertical flat plate. *Trans. ASME* **80**, 347–359.

Soundalgekar, V. M., Deka, R. & Das, U. N. 2003 Transient free convection flow of a viscous incompressible fluid past an infinite vertical plate with periodic heat flux. *Indian J. Engng Mat. Sci.* **10**, 390–396.

Zhao, T. S & Cheng, P. 1998 Heat transfer in oscillatory flows. *Annu. Rev. Heat Transfer* **9**, 359–420.